RESEARCH PROGRESS IN MECHANICAL AND MANUFACTURING ENGINEERING
e-ISSN: 2773-4765

RPMME

Vol. 5 No. 1 (2024) 259-268
https://publisher.uthm.edu.my/periodicals/index.php/rpmme

Fabrication and Physiochemical Properties of Alginate and Honey Biofilm for Wound Healing Applications

Fatin Amirah Yusop[1,2], Mohamad Hasshim Mohd. Sabirin[1,2], Maizlinda Izwana Idris[1,2]*,

[1] Department of Manufacturing Engineering, Faculty of Mechanical and Manufacturing Engineering, University Tun Hussein Onn Malaysia, Parit Raja, 86400, MALAYSIA
[2] Bioactive Materials (BioMA) Centre of Research, Faculty of Mechanical and Manufacturing Engineering, University Tun Hussein Onn Malaysia, Parit Raja, 86400, MALAYSIA

*Corresponding Author: izwana@uthm.edu.my
DOI: https://doi.org/10.30880/rpmme.2024.05.01.030

Article Info

Received: 30 January 2024
Accepted: 03 June 2024
Available online: 15 September 2024

Keywords

Biofilm, Alginate, Honey, Wound Healing, Scanning Electron Microscope, Fourier Transform Infrared Spectroscopy, Atomic Force Microscopy.

Abstract

This research about the fabrication and characterization of alginate and honey biofilms, exploring their potential applications in wound healing. Alginate wound dressings, derived from brown seaweed, are recognized for their notable features, such as high permeability, biocompatibility, moisture retention, and gel-forming capabilities. This research investigates the collaborative properties of alginate and manuka honey, a natural wound-healing agent renowned for its antimicrobial, anti-inflammatory, and antioxidant effects. The experiment uses the solution casting technique to create biofilms with varied alginate (1 gram to 2 grams) and honey concentrations (0 ml to 30 ml) crosslinked with 0.1% calcium chloride. Results acquired through Scanning Electron Microscope (SEM), contact angle measurements, Fourier Transform Infrared Spectroscopy (FTIR), and Atomic Force Microscope (AFM) illuminate how honey influences the biofilm's microstructure, surface roughness, and hydrophilicity. Elevated honey concentrations contribute to increased thickness, roughness, and porosity, impacting the overall structural integrity. The contact angle results affirm the hydrophilic nature of the biofilm surfaces, which is crucial for wound healing by enhancing moisture retention. SEM images vividly portray irregularities, including pores and rough surfaces, attributed to uneven drying and solidification processes. AFM analysis corroborates these findings by revealing higher surface roughness in the 2% w/v biofilm, aligning with SEM observations. FTIR spectra provide nuanced insights into the chemical composition of honey and its intricate interaction with alginate. The study posits that alginate and honey biofilms exhibit diverse compositions, showcasing their versatility for customized wound care applications. The confirmed hydrophilicity of these biofilms, coupled with their varied compositions, prompts further exploration of their behavior in interaction with host tissues. Ultimately, this research promising the role of alginate and honey biofilms in advancing for wound materials.

1. Introduction

Alginate wound dressings, derived from brown seaweed, have emerged as prominent tools in wound care due to their unique properties. Comprising polysaccharide fibers, these non-woven and non-glue cushions or strips offer high permeability and interact effectively with wound exudate and serum. Upon contact with the wound, alginate dressings absorb exudate and form a gel, promoting a moist environment crucial for enhancing cellular activities like migration, proliferation, and differentiation [1]. The gel also acts as a barrier, preventing excessive lateral wicking of exudate and reducing the risk of wound maceration. With an impressive absorptive capacity, alginate dressings can absorb up to 20 times their weight, making them valuable in managing wounds with high exudate levels.

Honey, a traditional wound-healing remedy, provides various therapeutic benefits. Its antimicrobial activity, primarily through hydrogen peroxide release, aids in bacterial elimination and infection prevention [2]. Honey's anti-inflammatory and antioxidant properties contribute to reducing inflammation and protecting cells involved in wound healing from oxidative stress. The energy source from honey's high sugar content supports cellular metabolism and tissue repair [3]. Additionally, honey's low pH creates an acidic environment inhibiting bacterial growth, and its low water activity hinders bacterial colonization by drawing moisture out of the wound.

This research aims to fabricate alginate and honey biofilms using the solution casting method and explore their physiochemical properties. The synergistic combination of alginate and honey presents a promising avenue for advancing wound care strategies, offering insights into biofilm development and potential applications in tailored wound healing.

2. Materials and Methods

2.1 Materials

Sodium alginate Sodium alginate powder (molecular weight of 198.11mol/g and CAS number of 9005-38-3), manuka honey (molecular weight of 180.16 mol/g) and calcium chloride (molecular weight of 147.01 mol/g and CAS number of 10035-04-8) are prepared. All materials stated are manufactured by SIGMA ALDRICH and can be found in the Fuel Analysis Laboratory. University Tun Hussein Onn Malaysia (UTHM).

2.2 Fabrication of alginate/honey biofilm

1% w/v solution of sodium alginate is meticulously prepared by adding the alginate powder gradually to 100 ml of distilled water. The solution is placed on a magnetic stirring hotplate, and continuous stirring for one hour ensures the prevention of clumping, resulting in the complete dissolution of the alginate powder and the formation of a homogenous solution. Subsequently, the alginate solution is blended with varying volumes of honey (0 ml, 5 ml, 15 ml, 20 ml, 25 ml, and 30 ml) through stirring for 30 minutes. Each blend is then carefully poured into three petri plates, covering the entire surface area. Following this, the samples in the petri dishes are left undisturbed for different durations—15 minutes, 30 minutes, and 1 hour—before the commencement of the crosslinking process.

Viscolite 700 was chosen to precisely assess the viscosity of the alginate/honey solution, offering vital insights into the solution's rheological characteristics in a simple and efficient way.

2.3 Characterization

Morphology Observation

A Scanning Electron Microscope (SEM) was used to examine the surface structure of the material. To increase electrical conductivity, dried biofilm was gold-coated. The image was then captured at a magnification of 1000x.

Functional Group Test

The functional group that exists from the spectrum was examined using Fourier Transform Infrared Spectroscopy (FTIR), which exhibits the structure of the components in the biofilm and the interaction between sodium alginate and manuka honey.

Contact Angle

Contact angle measurements were used to assess the surface wettability of alginate and honey films.

Surface Analysis

The alginate/honey surface topology was determined using a contact mode Atomic Force Microscope (AFM). The dried biofilm, about 1cm x 1cm, was adhered to the glass slide.

3. Results and discussions

3.1 Viscosity analysis

Viscosity is an important rheological parameter representing a fluid's resistance to flow. Understanding the parameters that influence viscosity in alginate and honey solutions is critical for optimizing formulations in a variety of applications. Table 1 presents viscosity values for various alginate and honey solution concentrations, allowing for a thorough examination of the factors influencing viscosity variations.

Table 1 *Viscosity values for alginate/honey solutions*

Sample	Viscosity (mPa.s)	
	1% w/v	2% w/v
SAH0	6.5	16
SAH5	7.2	19.5
SAH15	8.2	23.1
SAH20	8.9	28.8
SAH25	10.4	31.1
SAH30	11.7	37.5

The findings show a continuous increase in viscosity as alginate and honey concentrations increase from 1% w/v to 2% w/v. This association, which was detected in all samples, emphasizes the important role concentration plays in determining viscosity, which can be related to increased molecule entanglement or interactions. Notably, each sample formulation has distinct viscosity effects, with SAH30 exhibiting the maximum viscosity at both doses, implying a specific composition that contributes to greater thickness. The exact chemicals and amounts in this formulation are likely critical for producing the optimum viscosity for biofilm development, providing benefits such as better adhesion, stability, longer wound contact, and improved moisture retention, all of which are important for wound healing.

3.2 Surface morphology

The SEM pictures in Table 2 provide useful information on the morphological characteristics of biofilms under various circumstances.

Table 2 *SEM images of 1% w/v and 2 % w/v at the magnification of 1000X for (a) 1SAH0, (b) 2SAH0, (c) 1SAH5, (d) 2SAH5, (e) 1SAH15, (f) 2SAH15, (g) 1SAH20, (h) 2SAH20, (i) 1SAH25, (j) 2SAH25, (k) 1SAH30, (l) 2SAH30*

Magnification of 1000X	
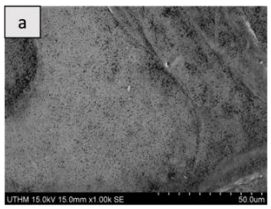 1SAH0	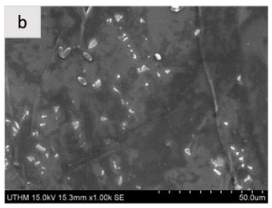 2SAH0
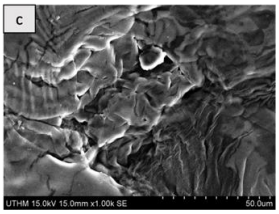 1SAH5	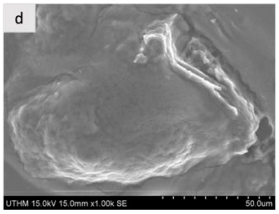 2SAH5

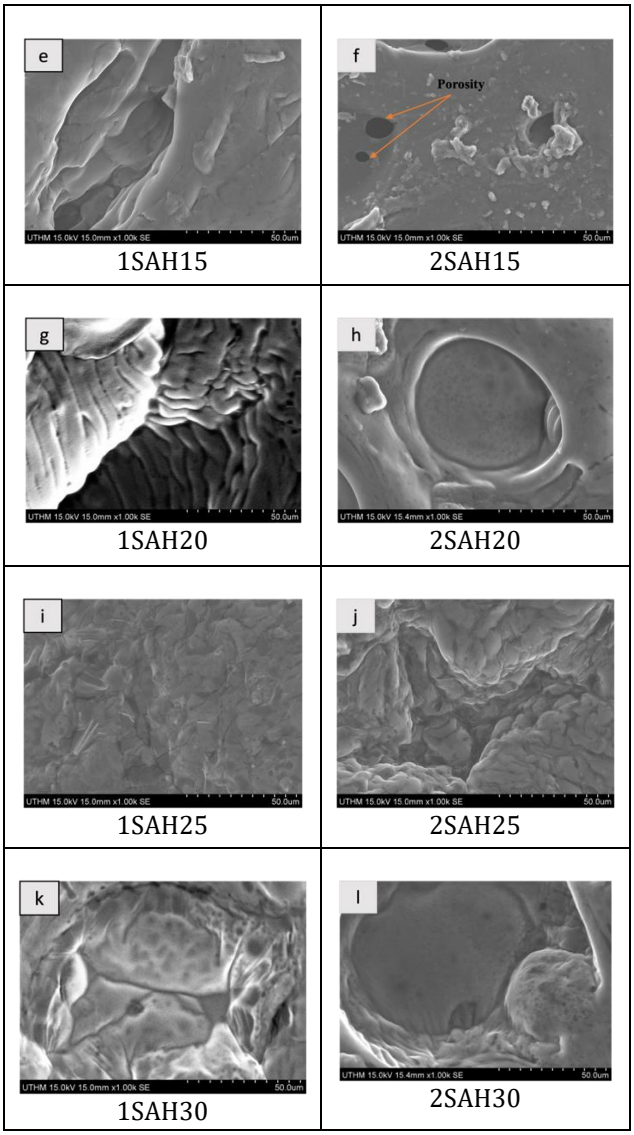

Image 1SAH0 shows a smooth and uniform surface, showing that biofilm production using alginate alone was effective. Image 2SAH0, while likewise displaying a flat surface, contains minute particles due to the difficulties of dissolving the thick alginate solution with calcium chloride. Images 1SAH5-2SAH30, on the other hand, show anomalies such as porosity, thick walls, rough surfaces, and bigger particles, which are attributable to the drying and mixing processes influencing biofilm solidification. As seen in the inconsistencies of 1SAH5-2SAH30, uneven drying during production can substantially affect surface properties, potentially producing in pores, visible walls, and a rough surface. The presence of bigger particles during the mixing phase may suggest unequal distribution or agglomeration.

3.3 Functional group analysis

The FTIR spectrum of sodium alginate exhibits distinct peaks corresponding to various functional groups within the biofilm. In Fig. 1 both spectra (a) and (b) reveal a prominent O-H stretching vibration peak at around 3339 cm-1, confirming the presence of hydroxyl groups in the polymer. Spectra (b) in the 2800-3000 cm-1 range display a peak at 2926 cm-1 associated with C-H stretching vibrations of aliphatic groups, which is not observed in spectra (a), suggesting that FTIR spectroscopy may be less sensitive to C-H stretching vibrations in aliphatic groups when their concentration is low in sodium alginate. Peaks in the 1600-1800 cm-1 range, corresponding to carbonyl (C=O) stretching vibrations of sodium alginate, are present in both spectra, associated with uronic acid residues. Additionally, both spectra exhibit peaks in the 1000-1200 cm-1 region, indicating the stretching vibration of C-O bonds, a common feature in polysaccharides like sodium alginate. This analysis underscores the unique features of the FTIR spectra and emphasizes the importance of considering sensitivity and concentration factors when interpreting C-H stretching vibrations in aliphatic groups. In comparison to prior research [4], FTIR spectrum of separated sodium alginate and standard, revealing distinctive peaks at 884 cm-1 and 939 cm-1

Research Progress in Mechanical and Manufacturing Engineering Vol. 5 No. 1 (2024) p. 259-268

associated with mannuronic acid and uronic acid, respectively. These peaks indicate the presence of monomers forming the polymer chain of sodium alginate, a polysaccharide derived from brown seaweed. The spectrum also highlights the presence of hydroxyl groups in sodium alginate, indicated by the OH functional group at a wavenumber of 3200-3400 cm-1, and CH2 stretching at 2924 cm-1, typically associated with the polysaccharide backbone.

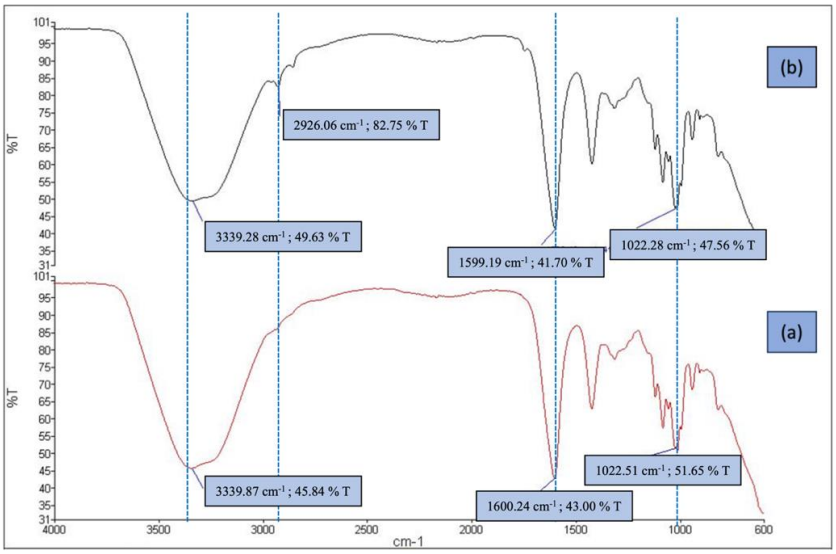

Fig. 1 *FTIR spectra for (a) 1SAH0, (b) 2SAH0*

Additionally, Fig. 2 and Fig. 3 depict FTIR spectra for different concentrations (1% w/v and 2% w/v) of sodium alginate with varying amounts of honey (5 ml, 15 ml, 20 ml, 25 ml, and 30 ml), all crosslinked with 0.1% calcium chloride. Both spectra share common features.

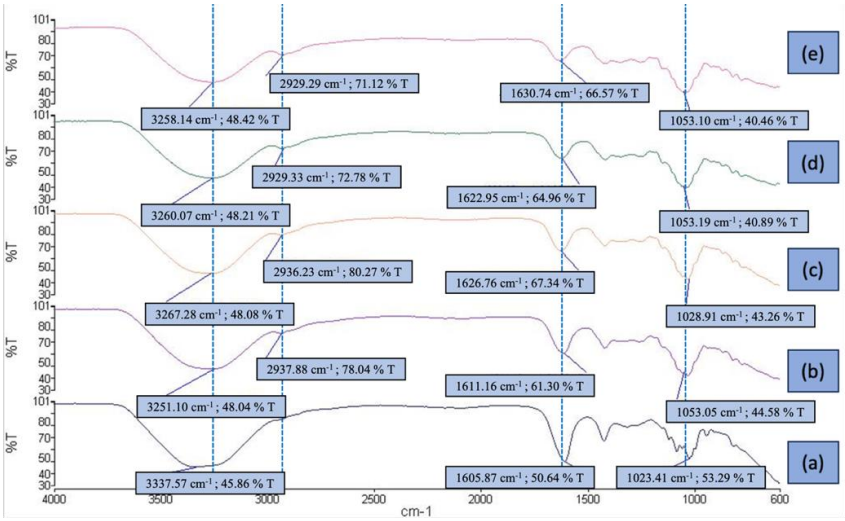

Fig. 2 *FTIR spectra for (a) 1SAH5, (b) 1SAH15, (c) 1SAH20, (d) 1SAH25, (e) 1SAH30*

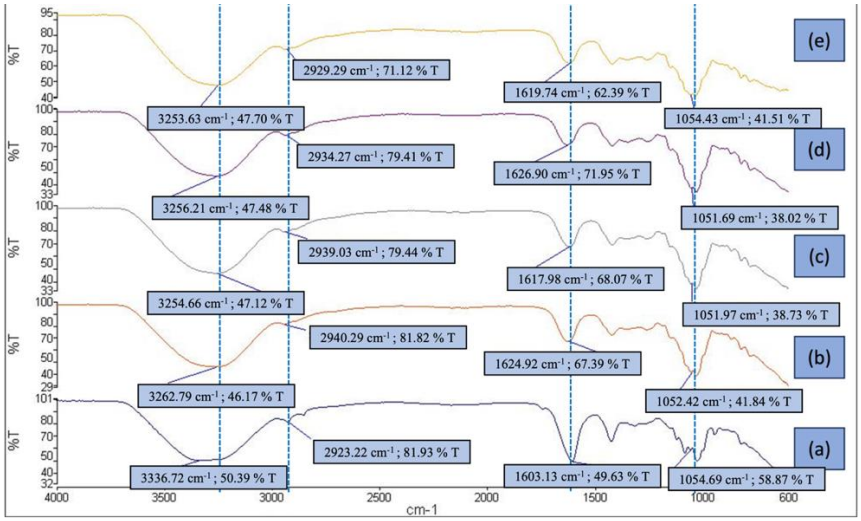

Fig. 3 *FTIR spectra for (a) 2SAH5, (b) 2SAH15, (c) 2SAH20, (d) 2SAH25, (e) 2SAH30*

According to [5], the O-H stretching vibration, evident as a prominent peak in the 3200-3600 cm-1 region, signifies the presence of hydroxyl groups, mainly associated with the water content in honey. Peaks in the 2800-3000 cm-1 range correspond to the stretching vibrations of C-H bonds in honey's aliphatic groups. The 1600-1800 cm-1 range includes peaks related to the stretching vibration of carbonyl (C=O) groups, likely originating from sugars and other honey constituents. The stretching vibration of C-O bonds, typical in carbohydrates and polysaccharides, is observed in the 1000-1200 cm-1 range. These spectral features collectively offer a comprehensive understanding of honey's chemical composition and its interactions with sodium alginate during calcium chloride crosslinking.

3.4 Contact Angle – Hydrophilicity (90°)

The surface wettability of alginate and honey films was assessed through contact angle measurements, as detailed in Table 3, which presents contact angle values for alginate and honey biofilms crosslinked with 0.1% calcium chloride at varying honey concentrations (0 ml - 30 ml). According to [6], contact angle measurements offer insights into the surface properties of hydrogels, with higher angles indicating reduced hydrophilicity, or lesser inclination to interact with water. The study observed that increasing honey concentration led to a decrease in hydrophilicity. Tables 3 and Table 4, presenting contact angle values for Alginate/Honey Biofilm at concentrations of 1w/v% and 2w/v%, enable comparisons of wetting behaviors and identification of variables influencing these values.

Table 3 *Contact angle values for alginate/honey biofilm (1%w/v)*

Sample	Contact Angle (°)		
	1st	2nd	Average
1SAH0	7.50	0	7.50
1SAH5	0	0	0
1SAH15	0	0	0
ISAH20	15.00	0	15.00
1SAH25	0	0	0
1SAH30	16.8	7.80	12.3

In Table 3, at 1w/v%, the contact angle for biofilm 1SAH0 with no honey is 7.50°, indicating a reasonably hydrophilic surface. Alginate alone contributes to some wetness. Samples 1SAH5, 1SAH15, and 1SAH25 show 0° contact angles due to porosity and surface roughness (refer to Table 4.2). Porous and rough surfaces tend to exhibit increased wetting characteristics, allowing liquid penetration and reducing contact angles. On the other hand, samples 1SAH20 and 1SAH30, with higher honey concentrations (20ml and 30ml), display larger contact angles (15.00° and 12.3°, respectively), indicating a balance between alginate and honey concentrations.

Research Progress in Mechanical and Manufacturing Engineering Vol. 5 No. 1 (2024) p. 259-268

Table 4 *Contact angle values for alginate/honey biofilm (2%w/v)*

Sample	Contact Angle (°)		
	1st	2nd	Average
2SAH0	31.80	27.50	29.65
2SAH5	20.50	0	20.50
2SAH15	17.70	0	17.70
2SAH20	15.00	0	15.00
2SAH25	0	0	0
2SAH30	14.10	0	14.10

In Table 4 (2w/v%), the biofilm 2SAH0, which contained no honey, showed a larger contact angle of 29.65° compared to the comparable 1w/v% sample, indicating a more hydrophobic surface influenced by the increased alginate concentration. Samples 2SAH5, 2SAH15, 2SAH20, and 2SAH30, with varying honey concentrations, exhibited contact angles ranging from 15.00° to 20.50°. The presence of honey contributed to hydrophilicity, with 2SAH30 displaying the most significant contact angle impacting wetting behavior.

3.5 Surface roughness analysis

The role of calcium chloride as a crosslinking agent in the development of alginate and honey biofilms with varying parameters was investigated using Atomic Force Microscopy (AFM). The surface roughness of alginate and honey biofilms with various concentrations of honey is shown in Table 5. As shown in Tables 6 and 7, the surface roughness of an alginate and honey biofilm was determined using the mean value of peak to valley roughness (Rpv), root mean square roughness (Rq), and average roughness (Ra) [7].

Table 5 *2D and 3D AFM images of 1% w/v and 2 % w/v alginate/honey biofilm for (a) 1SAH0, (b) 2SAH0, (c) 1SAH5, (d) 2SAH5, (e) 1SAH15, (f) 2SAH15, (g) 1SAH20, (h) 2SAH20, (i) 1SAH25, (j) 2SAH25, (k) 1SAH30, (l) 2SAH30*

Sample	1 w/v % Biofilm	2 w/v% Biofilm
SA	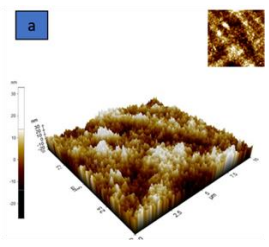	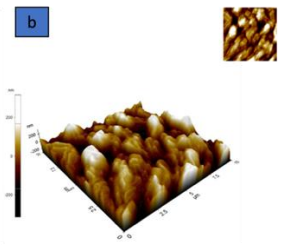
SAH5	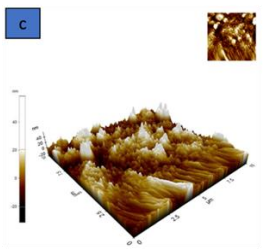	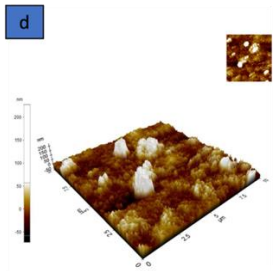

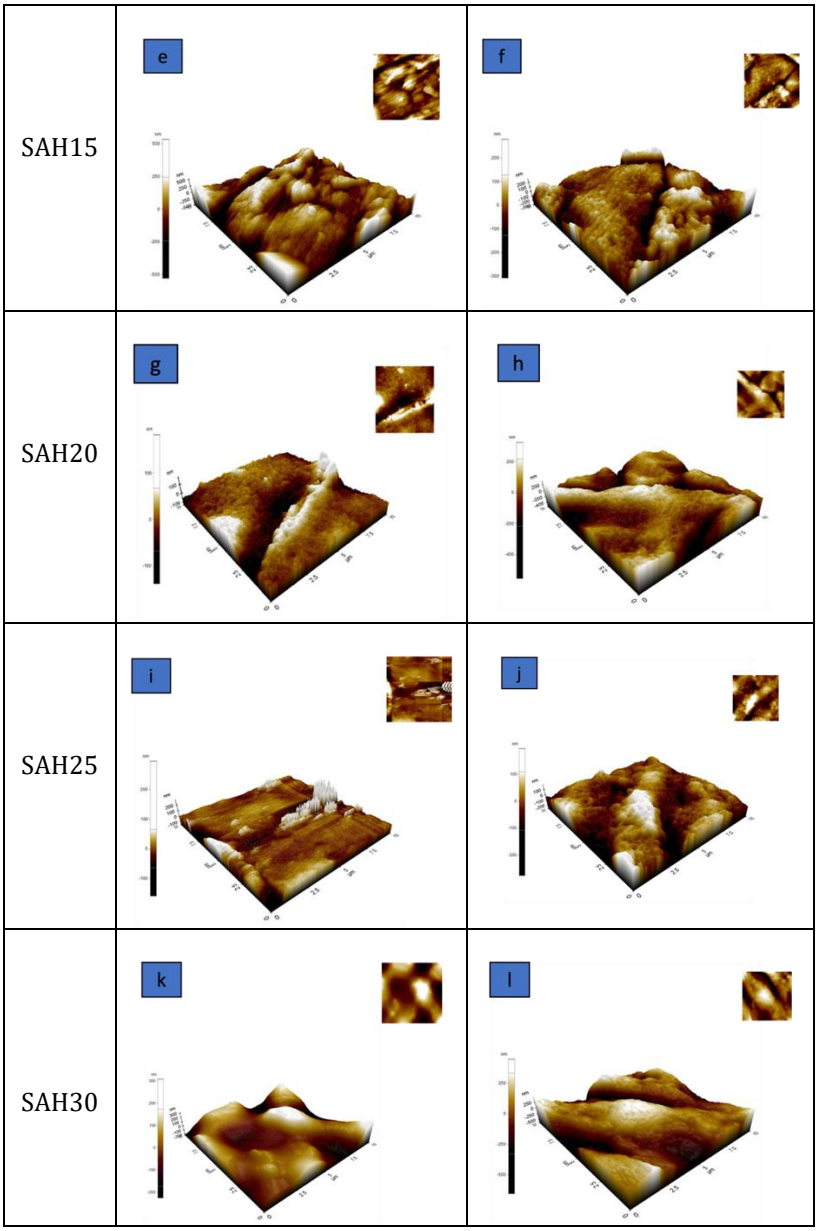

Table 6 *Surface roughness parameter for 1% w/v biofilm*

Sample	Surface Roughness		
	Rpv (nm)	Rq (nm)	Ra (nm)
1SAH0	59.820	7.093	5.597
1SAH5	89.819	10.456	8.012
1SAH15	1062.153	124.482	96.442
1SAH20	321.909	34.539	24.509
1SAH25	455.985	32.865	19.666
1SAH30	534.504	88.021	70.633

Table 7 *Surface roughness parameter for 2% w/v biofilm*

Sample	Surface Roughness		
	Rpv (nm)	Rq (nm)	Ra (nm)
2SAH0	630.750	85.521	66.816
2SAH5	299.841	29.164	19.242
2SAH15	588.279	65.332	49.122
2SAH20	881.344	111.003	85.522
2SAH25	469.978	55.495	42.152
2SAH30	1098.949	168.367	132.394

AFM analysis of surface roughness provides crucial insights into the topography of 1% w/v and 2% w/v alginate/honey biofilm samples, as detailed in Table 6 for the 1% w/v biofilm. Notably, 1SAH15 displays a significant increase in roughness, indicating a heterogeneous surface, possibly due to the combination of alginate and honey. In contrast, the other 1% w/v biofilm samples exhibit lower roughness values, with 1SAH0 displaying a uniform and smoother surface. Table 7, representing the 2% w/v biofilm, also shows changes in surface roughness parameters. Notably, 2SAH30 exhibits the highest roughness values, suggesting a textured and heterogeneous surface compared to other formulations. The elevated roughness in 2SAH30 may result from higher levels of alginate and honey, contributing to distinctive features. Comparing equivalent concentrations (1% w/v vs. 2% w/v), the 2% w/v biofilm generally exhibits higher surface roughness values, especially in samples with higher alginate concentrations, aligning with SEM image irregularities. The uneven drying and solidification process, influenced by higher solution viscosity, may lead to the formation of pores, thick walls, and rough surfaces, contributing to increased roughness values. Larger particles observed in SEM images may also contribute to elevated roughness values.

4. Conclusion

This research successfully fabricated alginate and honey biofilms using the solution casting method, investigating their physiochemical properties. Alginate was diluted in distilled water at 1% w/v and 2% w/v, combined with honey solutions at varying ratios, and biofilms were fabricated through solution casting and cross-linked with 0.1% calcium chloride. FTIR analysis revealed differences in bonding, affirming the hydrophilic nature of the biofilm surfaces observed in contact angle estimation. Low contact angles indicate strong water affinity, crucial for wound healing applications. SEM microstructure analysis showed that increasing honey and alginate concentrations increased biofilm thickness, roughness, and porosity. Irregularities observed in SEM images were linked to viscosity values, influencing uneven distribution during the mixing process. AFM analysis confirmed higher surface roughness in the 2% w/v biofilm, aligning with SEM observations. The versatility of alginate and honey in biofilm formation was demonstrated, with diverse compositions offering potential applications in wound healing. Physiochemical analyses, including FTIR, contact angle estimation, SEM, and AFM, provided comprehensive insights into molecular structure, hydrophilicity, microstructure, and surface roughness. Viscosity testing complemented characterizations, offering valuable data on fluid properties. In conclusion, this study successfully achieved its objectives, contributing valuable insights for potential applications of alginate and honey biofilms in wound healing.

Acknowledgment

This research was supported by the Ministry of Higher Education (MOHE) through Fundamental Research Grant Scheme (FRGS) (FRGS/1/2018/STG07/UTHM/02/6).

References

[1] S. Nasra, M. Patel, H. Shukla, M. Bhatt, and A. Kumar, "Functional hydrogel-based wound dressings: A review on biocompatibility and therapeutic efficacy," *Life Sciences*, vol. 334, p. 122232, 2023. doi: 10.1016/j.lfs.2023.122232

[2] S. Almasaudi, "The antibacterial activities of Honey," *Saudi Journal of Biological Sciences*, vol. 28, no. 4, pp. 2188–2196, 2021. doi: 10.1016/j.sjbs.2020.10.017

[3] H. Scepankova *et al.*, "Role of honey in advanced wound care," *Molecules*, vol. 26, no. 16, p. 4784, 2021. doi:10.3390/molecules26164784

[4] Helmiyati and M. Aprilliza, "Characterization and properties of sodium alginate from brown algae used as an ecofriendly superabsorbent," *IOP Conference Series: Materials Science and Engineering*, vol. 188, p. 012019, 2017. doi:10.1088/1757-899x/188/1/012019

[5] N. A. Azam and K. A. Amin, "Influence of manuka honey on mechanical performance and swelling behaviour of alginate hydrogel film," *IOP Conference Series: Materials Science and Engineering*, vol. 440, p. 012024, 2018. doi:10.1088/1757-899x/440/1/012024

[6] A. Mukhopadhyay *et al.*, "Dual cross-linked honey coupled 3D antimicrobial alginate hydrogels for cutaneous wound healing," *Materials Science and Engineering: C*, vol. 116, p. 111218, 2020. doi: 10.1016/j.msec.2020.111218

[7] R. Liu *et al.*, "Effects of beeswax emulsified by octenyl succinate starch on the structure and physicochemical properties of acid-modified starchfilms," *International Journal of Biological Macromolecules*, vol. 219, pp. 262–272, 2022. doi: 10.1016/j.ijbiomac.2022.07.235